IBIS/PICsIT

Instrument Specific Software (ISSW)

Report on the Scientific Performances of the PICsIT ISSW

Version: 1.1 – Date: 30 April 2003

Responsible: Luigi Foschini
IASF–CNR, Sezione di Bologna, (Italy)
and
INTEGRAL Science Data Centre, Versoix, (Switzerland)

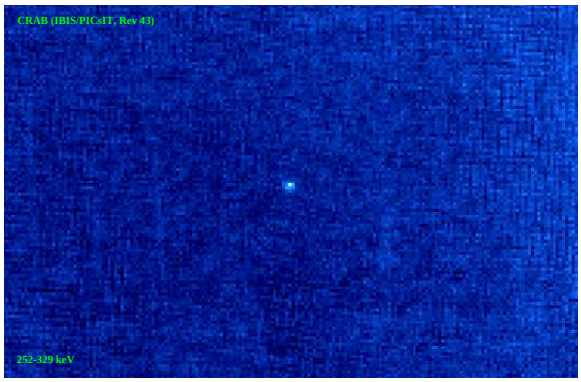

	Revision History
v 1.0	First version for first software release of March 2003
28/02/2003	
v 1.1	Update for the intermediate software release of May 2003
30/04/2003	Early analysis of Cyg X–1, cleaning of cosmic–ray induced events, improvement of the position accuracy, comparison with ECOE data.

Cover picture: Crab observed by PICsIT on 19 February 2003 for 132 ks in the energy band $252 - 329$ keV.

1 What is now available

This report summarizes the scientific performances and reliability of the Instrument Specific Software (ISSW) of the PICsIT detector layer of the IBIS imager. The executables analysed here are those officially delivered to date (30 April 2003), together with their Instrument Configuration (IC) files.

The PICsIT–ISSW delivered to date for the Scientific Analysis of the PICsIT data include:

- `ibis_pics_deadtime` (v 2.1, 23 October 2002): to calculate the intrinsic deadtime of the detector. It works well; no particular problem after the launch.

- `ip_ev_correction` (v 1.6, 14 November 2002): to perform a correction of gain and offset variations in addition to those performed on board by the Instrument Application Software (IASW). It is for data obtained in photon–by–photon mode. It is strilctly linked with the IC data structure PICS–ENER–MOD, containing the average gain, offset, and the deviations from these values pixel by pixel. The latest version of PICS–ENER–MOD is dated 30 October 2002 and was built by using the data in the IBIS Scientific Performance Report (IBIS Calibration Team, 2002). The exectuable is now stable and working. The only expected changes concerns the IC file, that should be updated with in flight data.

- `ip_ev_shadow_build` (v 2.2, 22 April 2003): to perform the building of the shadowgrams and the efficiency maps from data in photon–by–photon mode. It is stable and working. The only missing part is the treatment of the Good Time Interval (GTI); however, since the photon–by–photon mode is not the standard mode for PICsIT, and it was used only in exceptional cases during the PV phase with dedicated telemetry (because of the high background), the GTI inclusion is a low priority task. The executable is already ready to prepare shadowgrams also for the spectra extraction. Recently, the algorithm to clean the spurious events induced by cosmic-rays has been introduced (it works on `IBIS mode`= 43). See Sect. 2.2 for more details.

- `ip_si_shadow_build` (v 2.6, 20 March 2003): to perform the building of shadowgrams and the efficiency maps from the data in standard mode

(spectral imaging). It is stable and working. It is worth mentioning that the executable select only the complete histograms. If histograms are not complete, the executable returns no shadowgrams. It is foreseen, in the future, to deal also with partially complete histograms. The executable is already ready to prepare shadowgrams also for the spectra extraction.

- `ip_shadow_ubc` (v 2.4, 25 February 2003): to perform the correction for background and detector non–uniformities. The output shadowgrams are also expanded to take into account the gaps between modules. The gaps and the killed pixels are filled with a mean value. There is also a variance map, calculated starting from the statistical variance of the detector counts and updated according to the correction performed. The executable is linked with the following IC data structures: PICS–SBAC–BKG (background maps for single events), PICS–MBAC–BKG (background maps for multiple events), PICS–SUNI–BKG (detector non–uniformities for single events), and PICS–MUNI–BKG (detector non–uniformities for multiple events). See Sect. 2.1 for details.

- `ip_skyimage` (v 2.3, 18 March 2003): it performs the deconvolution and sky image reconstruction by means of the algorithm described by Goldwurm et al. (2001). The executable is working, producing a basic deconvolved sky image, variance, and significance maps. See Sect. 3 for details.

- `ip_st_lc_extract` (v 2.1, 16 April 2003): it performs the extraction of the lightcurve of the whole detector from the spectral timing data. The barycentric correction is applied, by using the library DAL3AUX. The executable is stable and working. The output files are in compliance with OGIP standards([1]).

- `Additional notes`: The executable for the Automatic Calibration Analysis (ACA) is not yet completed, because it is necessary to wait for an analysis of in–flight variations of the gains. After this analysis, it will be decided if this executable is necessary or not. The executables for the extraction of the spectrum and lightcurves from point–like sources are not yet ready. Work is in progress.

More details on some single items are in the following sections.

[1] See http://heasarc.gsfc.nasa.gov/docs/heasarc/ofwg/ofwg_recomm.html

2 The correction for background

2.1 Maps

There are no detector non–uniformities map available to date, except of one map created for test purposes (single events; no energy selection). The map is not to be used with the actual version of the ISSW, since it has been written with an old template, no more used. Using this map, can give wrong results and the crash of the pipeline. The removal of these maps from the archive has been requested.

For the background maps, the situation is different: there are three useful sets, prepared from the empty field observations of the revolution 13 (1 set for single and multiple events; 8 energy bands) and 38 (2 sets for single and multiple events; 8 energy bands). The differences in the two sets from the revolution 38 are due to a change in the energy bands.

PICsIT operates in an energy region dominated by the background, where we expect that the source counts are of the order of 1% of the global counts detected. This means that the background subtraction is of fundamental importance for the instrument capabilities.

The availability to date of only the empty field observations does not allow the user to be free to select the energy bands to produce images. A set of default energy bands has been created to have the best source statistics, with the lowest possible contamination from background or other events, such as the cosmic–rays induced events (see Segreto 2002). These energy bands, prepared by G. Di Cocco and G. Malaguti, are shown in Table 1.

A set of background maps corresponding to the energy bands listed in Table 1 have been created. No corresponding detector uniformity maps have been created, since a modelling activity is necessary to separate the contribution of the background from the detector non–uniformities. With the empty field observations is only possible to subtract the background. Nevertheless, this correction, although partial, is sufficient.

It is worth mentioning, as already seen in SIGMA calibrations and data reduction (Bouchet et al. 2001), that a background subtraction is more efficient when the background map is prepared from a nearby observation. This means that the background map generation is continuosly evolving. In addition, T. Bird is actually developing a parametric model, that will allow to the user the possibility to freely select the energy bands (Bird 2003).

Actually the executable contains two ways to rescale the background

Table 1: PICsIT Energy Bands. Columns: (1) Channel number in photon–by–photon mode; (2) Channel number in standard mode; (3) Energy [keV].

Channels PPM (1)	Channels Standard (2)	Energy (3)
Single Events		
29 – 35	10 – 16	203 – 252
36 – 46	17 – 27	252 – 329
47 – 64	28 – 41	329 – 455
65 – 94	42 – 56	455 – 655
95 – 150	57 – 84	655 – 1057
151 – 262	85 – 140	1057 – 1841
263 – 509	141 – 196	1841 – 3570
510 – 929	197 – 254	3570 – 6510
Multiple Events		
24 – 31	5 – 12	336 – 448
32 – 46	13 – 27	448 – 658
47 – 74	28 – 46	658 – 1050
75 – 130	47 – 74	1050 – 1834
131 – 254	75 – 136	1834 – 3570
255 – 464	137 – 187	3570 – 6510
465 – 679	188 – 229	6510 – 9520
680 – 929	230 – 254	9520 – 13020

maps: according to the time of exposure and to the average value of counts. Although a more detailed study is necessary, it appears that the average value scaling could give better results in searching for weak sources. However, this is still to be validated.

2.2 Cosmic–ray induced events

Since the beginning of the in–flight operations, it was clear that there were spurious events contaminating the detector in addition to the backgroud and source events([2]). The cause was identified in cosmic–ray induced events, that are roughly the 10% of the total events and affect mainly the energy bands below 300 keV (Segreto 2002, see also Natalucci 2003). As underlined by Natalucci (2003) these fake events can significanly affect the performances of PICsIT. However, it is possible to perform a cleaning only in photon–by–

[2]See some nice animations by the IBIS Team in Tübingen at http://astro.uni–tuebingen.de/groups/integral/anim_gif/.

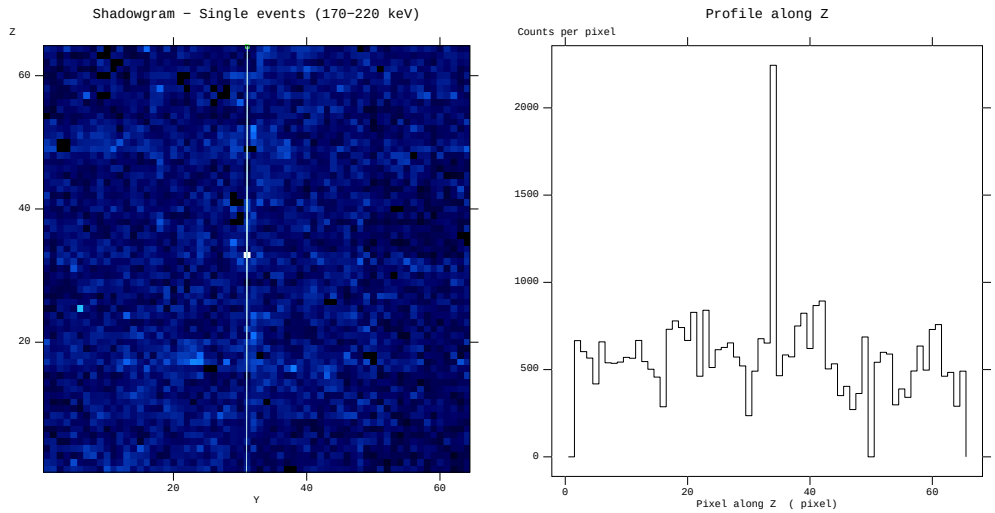

Figure 1: Effect of cosmic-rays induced events on the shadowgrams. The white pixels have an anomalous high count value. This example is taken from the data of revolution 24 in the energy band $170 - 220$ keV; PICsIT was in photon–by–photon mode.

photon mode. In standard mode, it is possible to perform only an *a posteriori* correction: when the pixel counts are higher than a constant multiplied by the average count values, i.e. $counts > k \cdot average$ (see Fig. 1), then it is assumed that this abnormal high value is due to a cosmic–ray induced event and the pixel value is reset to the mean value. First tests showed a certain effectiveness of this correction, but work is in progress to have a better solution, according to the casual nature of these events.

This hypothesis is confirmed by the analysis of photon–by–photon data: indeed, in this case, it was possible to develop an algorithm to delete from the photon list those events that can be identified as fake. After having isolated some of these "tracks", the photon list displayed series of photons "packed" in a very short time scale hitting a single pixel. Such "packets" are shown in Fig. 2, where fake events are emphasized in blue.

By removing these packets it is possible to obtain a cleaned shadowgram (Fig. 3), but obviously this is possible only when PICsIT is set to operate in photon–by–photon mode. Since the available telemetry is not sufficient for this type of operation, PICsIT will work almost always in standard mode,

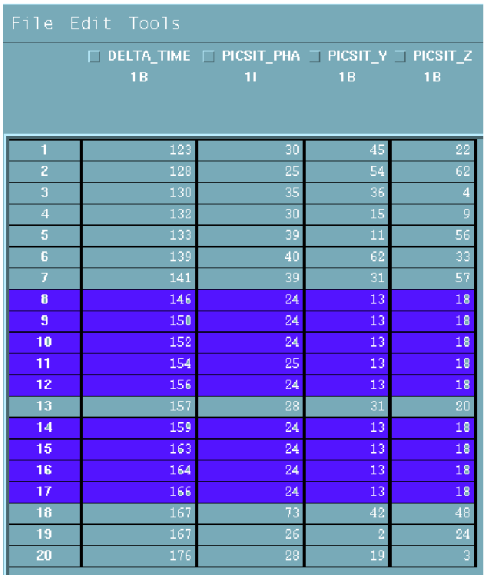

File Edit Tools

	DELTA_TIME 1B	PICSIT_PHA 1I	PICSIT_Y 1B	PICSIT_Z 1B
1	123	30	45	22
2	128	25	54	62
3	130	35	36	4
4	132	30	15	9
5	133	39	11	56
6	139	40	62	33
7	141	39	31	57
8	146	24	13	18
9	150	24	13	18
10	152	24	13	18
11	154	25	13	18
12	156	24	13	18
13	157	28	31	20
14	159	24	13	18
15	163	24	13	18
16	164	24	13	18
17	166	24	13	18
18	167	73	42	46
19	167	26	2	24
20	175	28	19	3

Figure 2: Identification in the photon list (single events) of fake events produced by cosmic–rays. Spurious events are emphasized in blue.

i.e. with events integrated onboard in histograms. In this way, there is no possibility to act on the single photon and it is possible only to operate the *a posteriori* correction described above.

3 The sky image reconstruction

3.1 Efficiency of the deconvolution - PSF

One of the most important points in the restoring of the sky image is the decoding pattern. The mask and the detector grid have different pitches: the mask is spaced by 11.2 mm, while the PICsIT pixel pitch is 9.2 mm. According to the type of algorithm used, it could be necessary to interpolate the decoding pattern obtained from the mask to the detector grid or *vice–versa*.

In the actual algorithm implemented in the PICsIT module, the decoding pattern is interpolated on the detector grid: in this way, we can save computer processing time. The interpolation is performed once, stored in an IC file

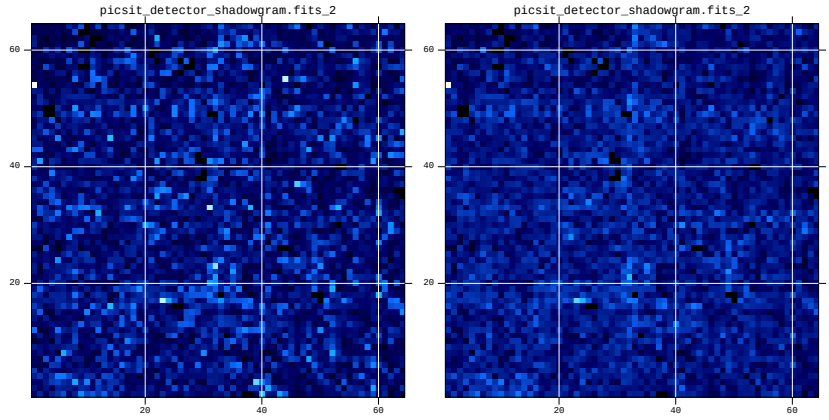

Figure 3: Effect of cosmic–rays induced events on the shadowgrams. (*left*) Normal shadowgram; (*right*) Cleaned shadowgram. After the cleaning, the bright pixels disappeared. The only bright pixel remained at the top left of the cleaned shadowgram is a well–known pixel that often is noisy. Data from revolution 14, energy band $170 - 250$ keV.

(PICS–DECO–MOD), and loaded when necessary. There are 5 decoding pattern now in the IC tree, but the present algorithm in `ip_skyimage` makes use of the decoding pattern n. 3.

The selected interpolation has a great impact in the efficiency of the deconvolution and several interpolation algorithms are now under study to select the best choice. The actual delivered version is based on a simple bi-linear interpolation and appears to give good and reliable results, as shown by the Point Spread Function in Fig. 4. With the actual hardware characteristics (mask and detector grid, etc...) the maximum significance in the PSF with a perfect interpolation is $\sigma \approx 47$; the actual available reaches $\sigma \approx 37$, corresponding to an efficiency of the deconvolution of about 79%. Work is in progress to improve the efficiency.

In addition, it is worth noting that the position of the source in the mask pattern (i.e. perfectly centered or not) can have impact in the reconstruction of the PSF, but this will be discussed in the next sections.

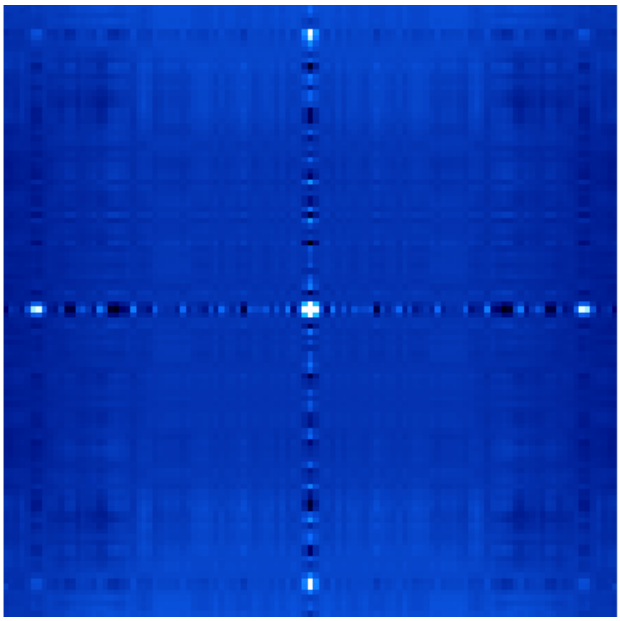

Figure 4: Point Spread Function of PICsIT with the decoding pattern interpolated with bilinear interpolation.

3.2 Sky coordinates reconstruction

The sensitivity of PICsIT does not allow to see sources during a typical exposure of one ScW ($2 - 5$ ks). It is necessary to integrate the shadowgrams to obtain long exposures of the order of $10^4 - 10^5$ s. This resulted to be problematic in realizing a detailed and extensive study of misalignement. To date, only three sources are available to test the sky coordinates reconstruction: they are Cygnus X–1 and Crab – in the FCFOV – and GRB021125 – in the PCFOV – (Bazzano and Paizis 2002).

The position of the Crab and Cygnus X–1 can be checked with the known catalog position, e.g. Simbad. For the GRB there can be the problem that the only position available with sufficient precision is that obtained with ISGRI (Gros and Produit 2002), the low–energy detector layer of IBIS, and there is the risk of self–reference. But the follow–up with other satellites of the GCN (GRB Coordinates Network) confirmed the position.

In the Table 2 are reported the positions found and the comparison with the other known coordinates. The three positions for the Crab are obtained

from the staring observation during the revolution 39 (Crab Star, 77 ks), from dithering osbervation of the revolution 43 (Crab Dith, 132 ks), and from Crab off–axis of 0.5° from the revolution 44 (Crab Off Ax, 104 ks). The position for Cyg X–1 is obtained from the dithered observation of revolution 11 (80 ks).

Table 2: Source position accuracy. Columns: (1) Source name; (2) Reference position (RA, Dec, J2000) from catalog or circulars; (3) PICsIT position (RA, Dec, J2000); (4) Offset [arcmin]. The position for PICsIT are taken in the $252 - 329$ keV energy band. The two positions for the GRB refers to that from the plain deconvolution (*Plain*) and that after the interpolation (*Int*).

Source	Reference Position	PICsIT Position	Offset
(1)	(2)	(3)	(4)
Cygnus X–1	$19:58:22; +35:12:06$	$19:58:08; +35:08:40$	$4.4'$
Crab Star	$05:34:32; +22:00:52$	$05:34:13; +21:55:48$	$6.8'$
Crab Dith		$05:34:24; +22:01:20$	$1.9'$
Crab Off Ax		$05:34:17; +21:59:11$	$3.8'$
GRB 021125 Int	$19:47:56, +28:23:28$	$19:47:46, +28:17:14$	$6.6'$
GRB 021125 Plain		$19:47:34, +28:15:13$	$9.5'$

The main conclusions from the position analysis are that the dithering gives a position generally better (we can expect this since to make the mosaic it is necessary to perform an interpolation) and it is better as the significance of the detection increases. The smallest offset is obtained with the Crab in dithering at 11σ level. The fact that PICsIT shows the best results in the energy band $252 - 329$ keV is due to the fact that this band is sufficiently low to have enough photons, but also sufficiently high to be not so much affected by the cosmic-ray induced events.

The worst cases are for the Crab in staring and for the GRB (but this is in the PCFOV). However, it is worth noting that one pixel of PICsIT corresponds to about $12'$, so that an offset of $6.8'$ corresponds to about half a pixel. This is the position after a basic deconvolution: it is foreseen to add a gaussian smoothing of the source to fit the peak, so to have a better positioning for staring observations and for the sources in the PCFOV.

It has been noted a little additional shift in the position of the Crab when detected at the highest energies, probably due to the increase of the mask transparency and, therefore, the coding is not complete.

4 Imaging with the calibration sources

4.1 Crab

The second part of the PV phase has been performed during February 2003. During the revolution 38 there were observations of empty field, useful for the background subtraction. Actually only about 13 ks (single events) and less than 9 ks (multiple events) of empty field observations were available and used to produce background maps (see Sect. 2). For the analysis with the Crab were selected the data from the revolution 39 (Crab on axis, staring, 77 ks), 43 (Crab on axis, dithering, 132 ks), and 44 (Crab off axis of 0.5°, dithering, 104 ks). The results are shown in the Table 3.

Table 3: PICsIT observations of the Crab during Rev. 39 (staring, on axis, 77 ks), Rev. 43 (dithering, on axis, 132 ks), Rev. 44 (dithering, off axis 0.5°, 104 ks). The columns indicate the energy band [keV], the count rate in the peak pixel [c/s] and the significance of the detection for each revolution.

	Rev 39		Rev 43		Rev 44	
Energy Band	Rate	σ	Rate	σ	Rate	σ
$200 - 252$	2.5	7.4	1.5	5.9	3.1	5.7
$252 - 329$	2.2	11.0	2.1	10.0	2.6	8.0
$329 - 455$	1.3	7.1	1.2	6.5	1.4	5.0
$455 - 655$	0.7	4.4	0.6	3.3	0.6	3.0

Monte Carlo simulations by Del Santo et al. (2001) are available for comparison, although in different energy bands (Table 4).

Table 4: Monte Carlo simulations of PICsIT observations of the Crab. Columns: (1) Energy band [keV]; (2) Count rate [c/s].

Energy Band (1)	Rate (2)
$150 - 250$	10
$250 - 400$	4.6
$400 - 1000$	2.1

The results of the revolution 39 were also confirmed by a software for the PICsIT imaging developed independently in Bologna by J.B. Stephen and

running on the same data structure (G. Di Cocco, personal communication, 2003).

The best performances of PICsIT are obtained in the energy band $252 - 329$ keV, that is less affected by the cosmic–rays induced events and is in a range sufficiently low to detect enough photons. In the Fig. 5-7 are shown the significance maps of the observation at $252 - 329$ keV, the best detection, together with the radial profile.

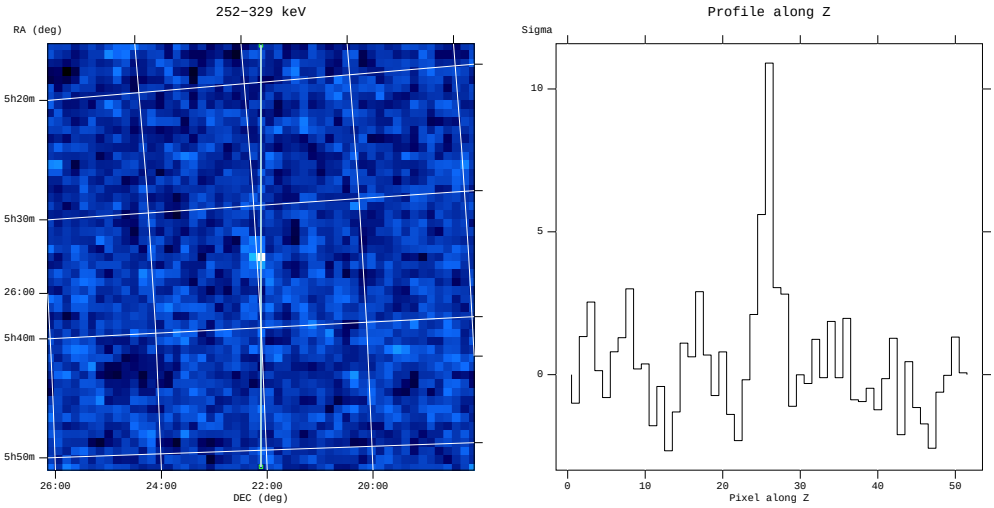

Figure 5: Crab observation during the rev 39 (staring, on axis, 77 ks). Significance map and profile in the energy band $252 - 329$ keV.

The greatest differences in the count rates and significance (for observations in staring, dithering, off axis) occur just the band $203 - 252$ keV, where we expect that the impact of cosmic–ray induced events is still high. In addition, we expect to have a degradation of the performances of the instrument when we change mode of observation (staring to dithering) or when we have the source off axis. To evaluate this, the three observations of the Crab (staring, dithering, dithering and off axis) have been normalized to the exposure of 132 ks (Table 5). Although it is expected that the value are a bit lower when passing from staring to dithering, since the mosaic performs an interpolation (pixels are not always perfectly aligned), this can account of only for a difference of 10%. Therefore, the greater differences shown in Table 5 are mostly due to other factors. The most probable cause is when

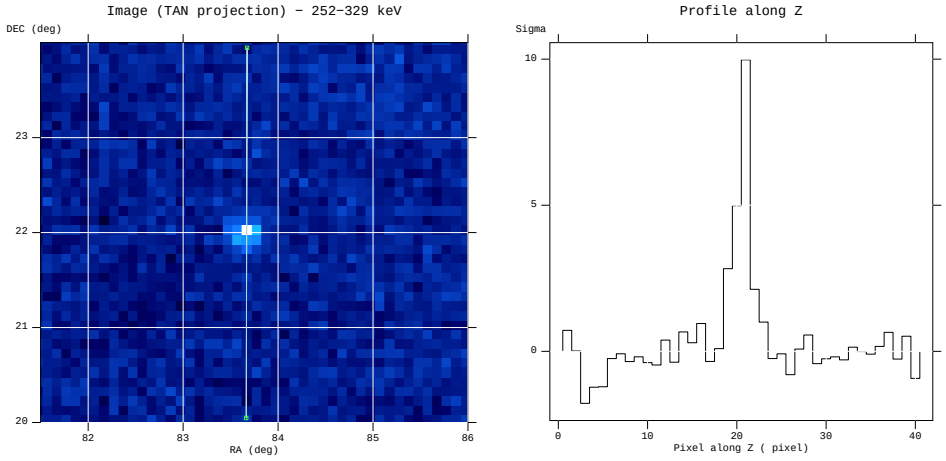

Figure 6: Crab observation during the rev 43 (dithering, on axis, 132 ks). Significance map and profile in the energy band $252 - 329$ keV.

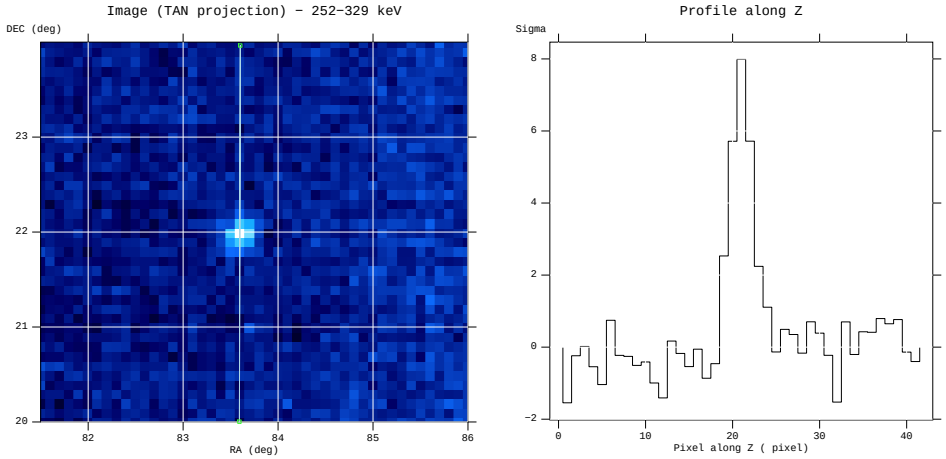

Figure 7: Crab observation during the rev 44 (dithering, off axis (0.5°), 104 ks). Significance map and profile in the energy band $252 - 329$ keV.

PICsIT is used in dithering, since IBIS has a mask best suited to work in staring. It is worth noting, that these are preliminary results and should be confirmed with more tests.

Table 5: PICsIT normalized observations of the Crab during Rev. 39 (staring, on axis, 77 ks), Rev. 43 (dithering, on axis, 132 ks), Rev. 44 (dithering, off axis 0.5°, 104 ks). The columns indicate the energy band [keV] and the significance of the detection for each revolution. The significance has been rescaled to the 132 ks of exposure of rev 43.

	Rev 39	Rev 43	Rev 44
Energy Band	σ	σ	σ
200 – 252	9.6	5.9	6.4
252 – 329	14.3	10.0	9.0
329 – 455	9.2	6.5	5.6
455 – 655	5.7	3.3	3.4

4.2 Cygnus X–1

Soon after the launch of INTEGRAL (17 October 2002), it was not possible to observe the Crab, since it was too close to the Sun. Therefore, Cygnus X–1 was selected as calibration source. The first observations started during the revolution 11 and PICsIT was in standard mode.

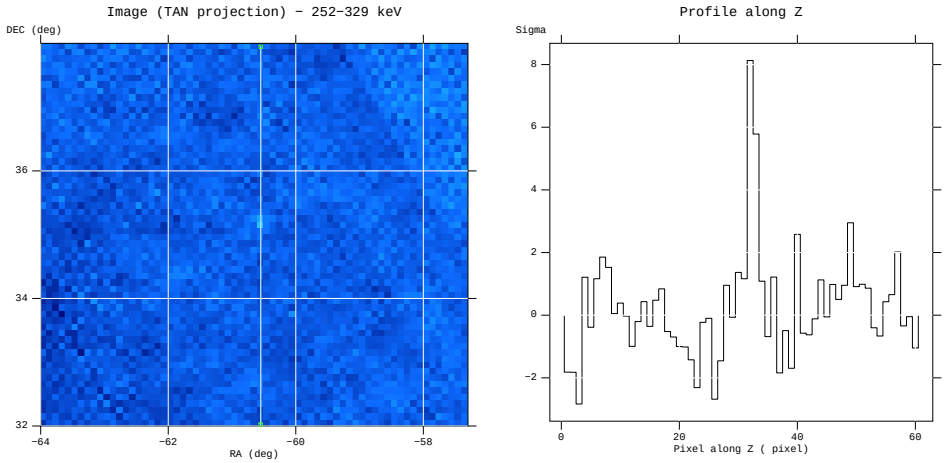

Figure 8: Cyg X–1 observed by PICsIT during the revolution 11 for 80 ks, dithering. Energy band 252 – 329 keV. Some background structures are clearly visible.

For other reasons, it was not possible to analyse immediately Cygnus X–1, but now – with the consolidated data – it is possible. To date the revolution

11 (80 ks, dithering) and 12 (13 ks, staring) have been analysed, with the detection of Cygnus X–1 in the first three energy bands of the observation in revolution 11. The 13 ks of the revolution 12 were not sufficient for a detection. The best detection is shown in Fig. 8. Since at that time there were several tests on the VETO configuration, the image is quite noisy, with fluctuations in the background. Nevertheless, the detection is clearly visible.

It is also possible to see that the PSF appears to be much more compact with respect to that of the Crab, but this can be due to the fact that the source was probably centered better.

These are only early results and a more detailed analysis will be soon performed.

5 Timing

In the Rev. 41, when the Crab was off–axis, PICsIT was in standard mode with the spectral timing set at about 1 ms of time resolution and four energy bands. A first weak detection of the pulse profile of the Crab is visible (Fig. 9). According to the Jodrell Bank monthly ephemeris of the Crab pulsar, the period is 0.03354548462 s measured on 15 January 2003. The best period found by PICsIT ISSW on a timescale of 2 Scw (exposure 8634 s) is 0.033548678 s, with some offset of the order of -10^{-6} s. Being the time resolution of 1 ms, this means that the differences found are at level of "numerical noise".

The detection is weak and it is expected to have better results with longer observations. It is worth noting that actually the barycentric correction is implemented, but not yet fully tested. Work in progress.

6 Additional tools

6.1 OSM

There are also three executables for the Operating Status Monitoring (OSM) in standard mode (spectral imaging, spectral timing) and photon–by–photon mode. They produce some standard products to monitor the instrument performances, that are shadowgrams, spectra and lightcurves for the whole detector, statistical analysis on the shadowgrams (mean value, maximum,

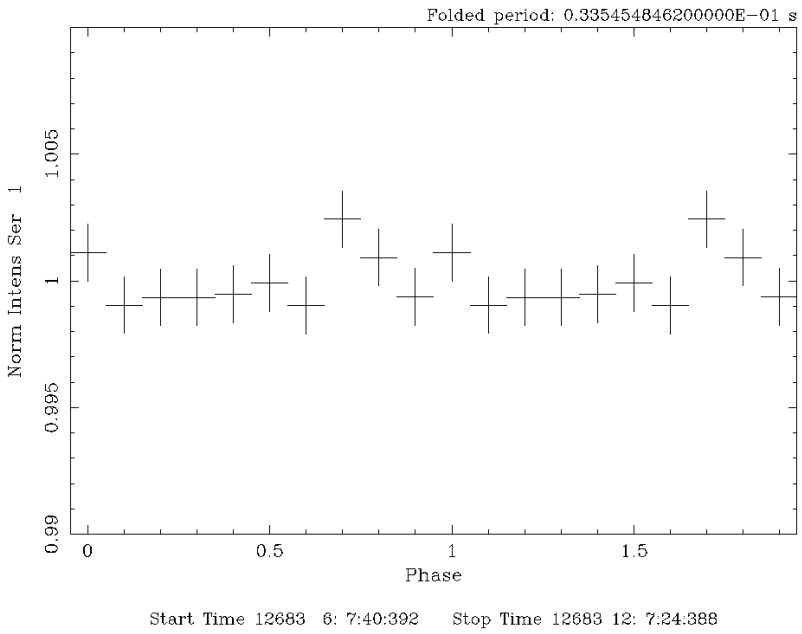

Figure 9: Pulse profile of the Crab in the energy band $260 - 364$ keV. The peak at high energy is visible. The time of observation is about 16 ks.

minimum, standard deviation). They are all working and stable. They are already used for the Consolidated Data Processing.

6.2 Background maps

An executable was developed to generate the background maps from empty field observations. Although, it is not intended for the common user, it is developed following the ESA and ISDC Coding and Testing Standards, so that, if necessary, it can be integrated in the usual ISDC pipelines. The executable is stable and working fine. The background maps available in the IC data base have been generated by means of this executable.

7 Non–standard analysis tools

7.1 Analysis of Gamma–Ray Bursts

In some particular cases, like the detection of GRB when PICsIT is in photon–by–photon mode, it could be necessary to extract the data with non–standard procedures. In normal conditions this is not possible. Indeed, by taking into account that PICsIT will work for almost its "life" in standard mode([3]), a GRB of tens of seconds will be lost in an histogram of thousands of seconds([4]). But, if PICsIT is in photon–by–photon mode, it is possible to extract the photon list of a selected time region and to perform the scientific analysis.

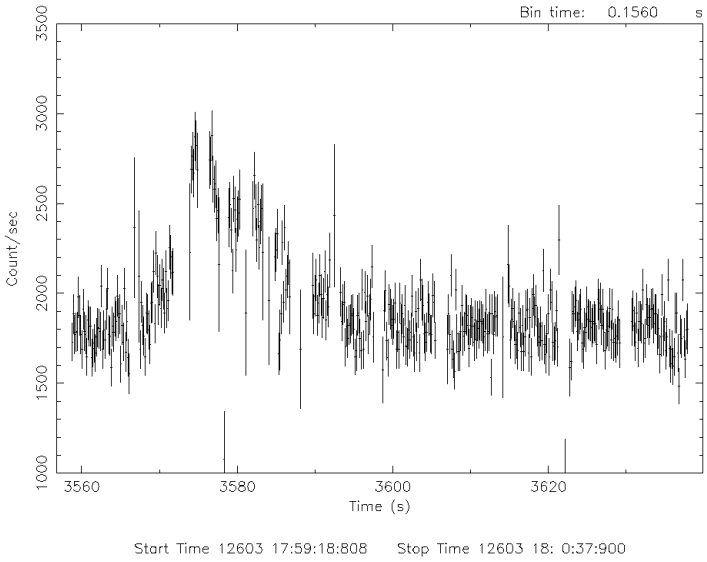

Figure 10: GRB021125: lightcurve of single events rebinned to 0.156 s The telemetry gaps are clearly visible.

[3]The actual telemetry is not sufficient to fulfill the request of the high count rate. Even with special configuration giving to PICsIT the maximum of telemetry and a reduced number of channels – as for the the experimental tests during which the GRB occurred – the gaps in the telemetry are clearly visible in Fig. 10.

[4]However, it is worth noting that in standard mode PICsIT has the spectral timing submode, that allows to get the lightcurve for the whole detector in two energy bands. In case of a strong GRB in the FOV it is expected to detect something.

While for imaging it is possible to use the usual executable (`ip_skyimage`), the extraction of the spectrum and the lightcurve requires a dedicated software. Some tools have been developed for the analysis of the GRB021125 (Bazzano and Paizis 2002), the first GRB seen by IBIS, during which PICsIT was in photon–by–photon.

The GRB has a high throughput of photons for a very short time and it well surpass the background count rate (see the lightcurve of the whole detector in Fig. 10). So that, if we consider the photons of the whole detector when observing the GRB and we subtract the background from an empty field observation, it is possible to extract a spectrum of the GRB (Fig. 11). The results obtained with the GRB021125 have been compared with those obtained by IBAS both for ISGRI and SPI–ACS, with the help of G. Malaguti, S. Mereghetti, J. Borkowski, and D. Götz. Results are consistent.

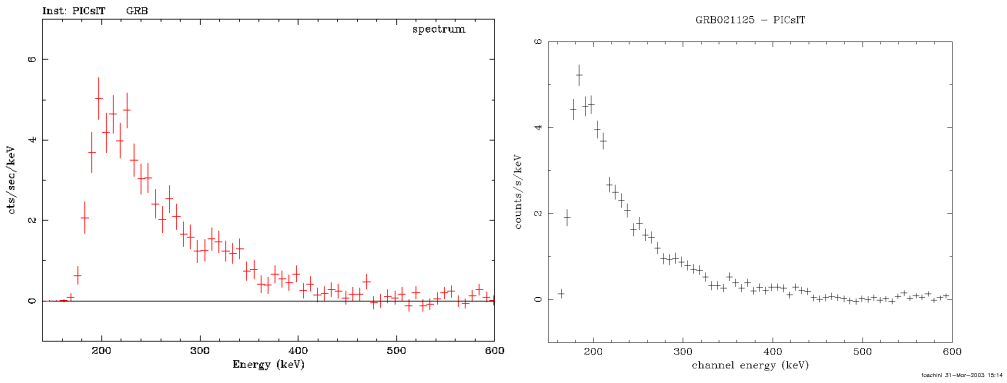

Figure 11: GRB021125: count spectrum from ECOE (*left*) and from ISSW (*right*). The spectrum from ISSW was rebinned to group min 30, while the ECOE one was not rebinned. The spectrum from ECOE was provided by A. Segreto.

In addition, the GRB021125 has been used to check if the data in output from the ISDC preprocessing and the ISSW are compatible with those from Experiment Check–Out Equipement stations (ECOE). In Fig. 11 the count spectra from ECOE and ISSW are shown and compared. The agreement is evident.

Two exectuables have been developed for this purpose and even though they are not intended for the standard pipeline, they are already suitable to became available for the users, since they are developed following the ESA

and ISDC Coding and Testing Standards.

7.2 Image mosaic

There is a tool by ISDC to make mosaics (`image_mosaic`), but at the time of the tests described in the present report, it was not working. Therefore, it was used an executable developed by M. Revnivtsev to work on ISGRI data and modified by myself to use PICsIT images. With the kind permission of the author.

8 Other sources analysed

In addition to the calibrations sources, some other tentatives have been done to detect other sources:

- *3C273:* it is an AO1 observation (PI: Courvoisier) and it was performed in early January (Rev 28, 30, and 32; staring and dithering). However, at that time there was VETO not correctly configured (particularly VETO bottom was off), so that the observation is strongly affected by the background. For this reason, most of the histograms are not complete (about 87%) and therefore discarded. The remaining exposure was not sufficient to get any detection.

- *Cyg X–3:* it was an observation for calibration (rev 23). Almost all the revolution was analysed, both for images and lightcurve. Nothing was detected. This can be explained by the fact that the source was in a very soft state: SPI spectrum arrives up to $150 - 200$ keV.

- *GRS 1915+105:* there was a ToO from ISWT in early April (rev 57, dithering) for about 100 ks, when the source had a soft spectrum ($\Gamma \approx 3$). No detection was found, but in the near–real time data about 10 Scw were not processed, while 6 other contained histograms not complete. Therefore, about 30 ks of observation were not available and the remaining 70 ks were not sufficient for a detection. With the consolidated data should be possible to recover the missing exposure and to try again to get a detection, although the very soft spectrum suggests that it will be clearly difficult to detect the source at high energy.

9 References

Please note that the IBIS internal reports are available at `http:ibis.ias.rm.cnr.it`.

- Bazzano A., Paizis A., 2002, GCN1706
- Bird A.J., 2003, *PICsIT Uniformity Modelling by Parametric Model.* IBIS Internal Report.
- Bouchet L. et al., 2001, ApJ 548, 990.
- Del Santo M. et al., 2001, AIP Conference Proceedings **587**, 826.
- Goldwurm A. et al., 2001, Proceedings of the IV INTEGRAL workshop, ESA **SP–459**, p. 497.
- Gros A., Produit N., 2002, GCN1714
- IBIS Calibration Team, *Scientific Performance Report*, IN.IB.IAS.RP.008/02, March 2002.
- Natalucci L., 2003, *Performance of S7.0 mode: preliminary results.* IN.IB.IASF/Rm.RP.0032/03, March 2003.
- Segreto A., *The cosmic–ray induced events on PICsIT*, IN.IB.IASF/Pa.RP.030/02, November 2002.